

Peptides Complexed to Cyclodextrin Fragment Rather than Dissociate When Subjected to Blackbody Infrared Radiation

Sharron G. Penn, Fei He, and Carlito B. Lebrilla*

Department of Chemistry, University of California, Davis, California 95616

Received: April 14, 1998; In Final Form: August 17, 1998

Blackbody infrared radiation dissociation is used to probe the fragmentation behavior of peptide–cyclodextrin complexes. Complexes formed by combining bradykinin (and some of its analogues) with permethylated β -cyclodextrin undergo peptide fragmentation rather than complex dissociation under these conditions. Activation energies and preexponential factors are obtained from Arrhenius plots constructed over a temperature range (between 323 and 440 K). The fragmentation behavior of the peptides does not differ considerably when the sites of inclusions are removed from the peptide. Molecular dynamics simulations are performed to better understand the experimental observations.

Introduction

The observation of noncovalently bound complexes in the gas phase has prompted mass spectrometric studies of their intrinsic stabilities in order to develop a rapid method for identifying and characterizing these complexes.^{1–7} Although many of these studies have involved large biomolecules, a large class of noncovalently bound complexes involve inclusion complexes of cyclodextrins. These complexes are important in separation chemistry and pharmacology.^{8–17} A previous study in this group has used heated capillary dissociation (HCD) and on-resonance collision-induced dissociation (CID) to study cyclodextrin–peptide complexes.¹⁸ Complexes of four peptides including bradykinin (BK, Arg-Pro-Pro-Gly-Phe-Ser-Pro-Phe-Arg), des-arg¹-bradykinin (dR1BK), des-arg⁹-bradykinin (dR9BK), and [glycine⁵, glycine⁸]-bradykinin (GGBK) with permethylated- β -cyclodextrin (CD) were studied. CID and HCD produced the same ordering of complex stability with regard to dissociation. The strength of interaction followed the order dR9BK < BK < dR1BK \approx GGBK. This suggested that the absence of Arg-9 destabilized the complex while the absence of Arg-1 stabilized the complex. Replacing both Phe residues with Gly similarly strengthened the peptide–cyclodextrin interaction, suggesting that the Phe residues destabilized the complex. We further concluded that the formation of inclusion complexes while a stabilizing feature in the solution is probably a destabilizing feature in the gas phase.

Multiphoton dissociation provides another method for studying the intrinsic interactions in noncovalently bound complexes. Multiphoton infrared radiation provides the lowest fragmentation pathway to dissociation. McMahon and Dunbar showed that the dissociation of weakly bound cluster ions stored in an ICR cell undergoes dissociation from absorption of blackbody radiation from the vacuum chamber.^{19,20} Williams illustrated the application of this photodissociation method (termed blackbody infrared radiative dissociation, or BIRD) on peptides and proteins as a method of tandem mass spectrometry. With the use of Fourier transform ion cyclotron resonance spectroscopy (FTICR) they determined rate constants that provided activation energies and the preexponential factors for the dissociation reactions.^{21,22} The ease of use of this method (heating the chamber is sufficient) and its ability to provide important

thermodynamic and kinetic information may make this an important tool for studying noncovalently bound complexes.

In this paper, we use blackbody radiation to study the dissociation of noncovalent cyclodextrin–peptide complexes. For this study, five peptides were chosen including bradykinin (BK), [Lys¹]-bradykinin (LBK, Lys-Pro-Pro-Gly-Phe-Ser-Pro-Phe-Arg), GGBK, dR1BK, and dR9BK. The compound LBK is a bradykinin analogue with the Arg-1 residue replaced by lysine. This compound was chosen to observe the effects of a less basic charge site on the fragmentation behavior of the complex. GGBK is also a BK analogue, where the Phe residues on positions 5 and 8 are replaced by glycines. It was chosen to observe the effects of eliminating the Phe inclusion sites. dR1BK and dR9BK are also analogues of BK with the Arg residues removed on positions 1 and 9, respectively. These compounds allow us to observe the effects of removing fixed charge sites on the peptides.

Experimental Section

Heptakis-tri-O-methyl- β -cyclodextrin (CD) and all the peptides except GGBK were obtained from Sigma Chemical Company (St. Louis, MO) and used without further purification. The [glycine⁵, glycine⁸]-bradykinin was synthesized for this project by Biosynthesis Inc. (Lewisville, TX). The electrospray solutions were prepared by dissolving equimolar amounts of peptide and cyclodextrin in 50:50 methanol/water solvent, each at a concentration of 2.0×10^{-5} M.

The electrospray ionization experiments were carried out on a home-built 3 T external source Fourier transform mass spectrometer and described in detail in previous publications.^{23–25} Briefly, the ions are produced and travel through a desolvation capillary that points toward a skimmer. The skimmer opens into a second chamber, maintained at 30 mTorr, which houses a second skimmer. The second skimmer opens into a chamber pumped by a turbo pump to a pressure of around 10^{-5} Torr. The ions are guided from the second skimmer into the opening of the quadrupole rods by a set of einzel lenses. The quadrupole rods extend through two differentially pumped chambers and end at the analyzer cell that is maintained at 1×10^{-9} Torr.

The analyzer chamber was heated by a large Watlow (St. Louis, MO) silicon heater that covered most of the analyzer

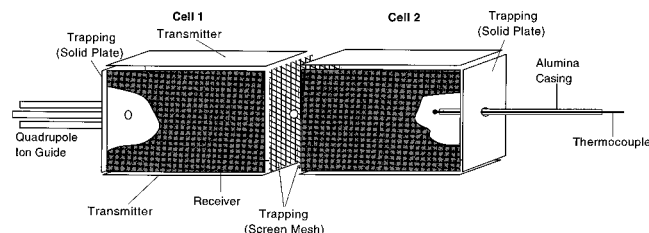


Figure 1. Analyzer cell used for BIRD experiments. Ions are trapped in cell 1 while the temperature is measured in cell 2 during the experiment. Ions are produced by ESI and guided in analyzer cell by a single set of quadrupole rods.

chamber, powered by a Hewlett-Packard (Rockaway, NJ) 6675A power supply to a series of temperatures between 90 and 170 °C. Higher temperatures were not attempted as their effects on the internal preamp were not known. The pressure during the dissociation experiment was typically around 1×10^{-8} Torr, well below the conditions typically used for collisional excitation. The dissociation of the complexes was measured as a function of residence time in the ICR cell. The doubly charged complexes were mass selected and allowed to dissociate. The rate constants were obtained from the slope using the equation

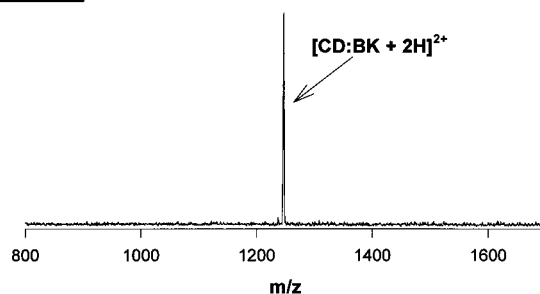
$$\text{slope} = \ln \frac{I_{[\text{CD:P+2H}]^{2+}}}{I_{[\text{CD:P+2H}]^{2+}} + I_{[\text{F}]}}$$

where $I_{[\text{CD:P+2H}]^{2+}}$ is the intensity of the double-charged peptide (P)–cyclodextrin (CD) complex and $I_{[\text{F}]}$ is the sum intensity of all the fragments, both singly and doubly charged.

The analyzer cell is composed of a double-cell design built for the manipulation and storage of multiple ion populations (Figure 1). It contrasts with the dual cell available in some commercial instrument in that it contains two complete analyzer cells. The two cells are further placed in the same vacuum chamber. The two analyzer cells are held in place by a set of MACOR spacers and placed at the end of a single-stage quadrupole ion guide. The solid plates are made of polished stainless steel. Although all the electrodes of both cells may be connected to the data system, in the present configuration the transmitter and receiver plates of cell 1 are connected to the data system while the corresponding plates for cell 2 are grounded. In addition, cell 2 was fitted with a thermocouple wire holder. This consists of a mounting assembly that holds in place a K type thermocouple wire inserted into a ceramic tube. The thermocouple was placed in the center of cell 2. The wire meshes allowed similar photodissociation conditions in the two cells. Care was taken to ensure that the thermocouple was not heated by its contact with the analyzer chamber through the feed-through connections.

Molecular Dynamics Simulations. Calculations were performed on a Silicon Graphics Indigo (Mountain View, CA) with the Insight II program from Biosym Technologies (San Diego, CA) using the CVFF force field. Molecular dynamics calculations were first performed by optimizing the separated peptide and cyclodextrin. The molecules were combined by, initially, including the Phe⁵ into the cavity and heating the complex to 600 K for 400 ps (calculation 1). At this temperature, a structure was captured every 8 ps resulting in 50 structures. Each structure was further annealed in 100 K increments for 50 ps at each temperature to 300 K, and the resulting structure was minimized to 0 K. The lowest energy structures of calculation 1 were found to have similar features, the most important being that Arg¹ is included in the cavity to replace Phe⁵. Similar

(a) 0 seconds



(b) 40 seconds

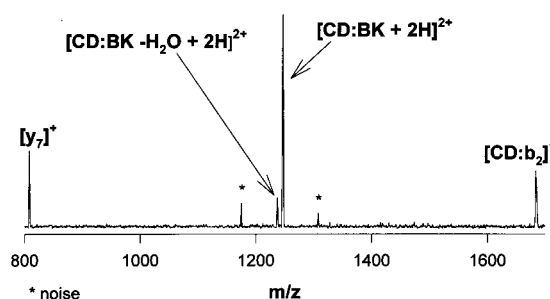
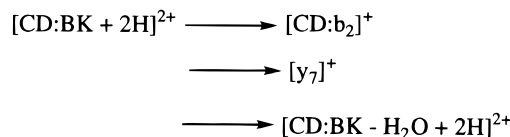


Figure 2. Spectrum of isolated complex $[\text{CD:BK} + 2\text{H}]^{2+}$ at 148 °C after a trapping period of (a) 0 s and (b) 40 s. The peaks labeled by asterisks are noise. The only fragments observed correspond to the loss of H_2O , $[\text{CD:b}_2 + \text{H}]^+$, and $[\text{y}_7 + \text{H}]^+$.

SCHEME 1: Fragmentation of $[\text{CD:BK} + 2\text{H}]^{2+}$ under BIRD Conditions



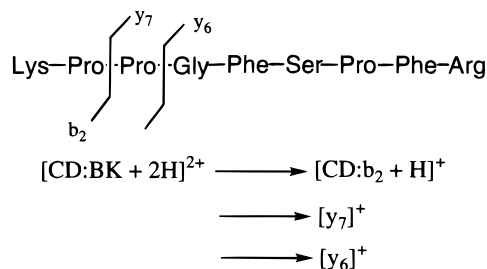
calculations were performed starting with Phe⁸ included in the cavity (calculation 2). The lowest energy structures of the resulting simulations maintained the inclusion of Phe⁸. To obtain the relative energy of the Phe⁵-included complex, the Phe⁵-included structure was recalculated by heating the structure to only 300 K for 400 ps (calculation 3). Each structure was minimized to 0 K, and the resulting low-energy structures maintained the inclusion of Phe⁵.

Results

Photodissociation of Peptide Cyclodextrin Complexes.

Figure 2a shows the spectrum of the isolated complex $[\text{CD:BK} + 2\text{H}]^{2+}$ at 148 °C. After a 40 s reaction period (Figure 2b), fragment ions are observed corresponding to loss of water $[\text{CD:BK} - \text{H}_2\text{O} + 2\text{H}]^{2+}$ and a complimentary cleavage pair corresponding to cleavage of the Pro–Pro bond $[\text{BK} - \text{ArgPro} + \text{H}]^+$ (or $[\text{y}_7]^+$) and $[\text{CD:ArgPro} + \text{H}]^+$ (or $[\text{CD:b}_2]^+$) (Scheme 1).

Both the loss of water and cleavage at the Pro residues are common fragmentation pathways of isolated protonated peptides.²⁶ As the cyclodextrin is fully methylated, the H_2O likely comes directly from the peptide at either the C-terminus and/or the serine residue. The absence of the doubly charged BK, $[\text{BK} + 2\text{H}]^{2+}$, and the presence of the peptide fragment complexed to cyclodextrin in the mass spectra further suggest that the fragments originate directly from the complex and not from an isolated $[\text{BK} + 2\text{H}]^{2+}$ ion. (For clarity and unless otherwise noted, dissociation will refer to the separation of the peptide guest and the cyclodextrin host, while fragmentation will refer

SCHEME 2: Fragmentation of $[\text{CD}:\text{LBK} + 2\text{H}]^{2+}$ under BIRD Conditions


to the cleavage of covalent bonds.) The nearly equal relative abundances of $[\text{y}_7]^+$ and $[\text{CD}:\text{b}_2]^+$ further support this notion. The lack of fragments resulting from the fragmentation of the cyclodextrin indicates that proton transfer from the peptide to the cyclodextrin is not a major process during the dissociation. Glycosidic bonds are highly labile when protonated and readily fragment.^{27–29} The results suggest that the proton is sequestered in the peptide despite the intimate contact between the two molecules. Furthermore, the fragments reveal the localized nature of the charges—each arginine residue binds a proton that remains strongly bound even after the peptide fragments.

The results of the BIRD experiments contrast with the earlier CID results where the dissociation of the complex produces the intact peptide.¹⁸ The CID of the $[\text{BK}:\text{CD} + 2\text{H}]^{2+}$ complex produces only trace amounts of the peptide fragments observed in BIRD. Instead, the dissociation of the complex is more highly favored to produce $[\text{BK} + 2\text{H}]^{2+}$ even with translational energies corresponding to the dissociation thresholds. Evidently, CID places more energy in the complex than BIRD so that even low-energy CID does not necessarily produce the lowest dissociation pathway. Instead, dissociation proceeds through the entropically favorable dissociation of the complex rather than the enthalpically favored process of peptide fragmentation.

The products of the $[\text{CD}:\text{BK} + 2\text{H}]^{2+}$ complex are fragments that are analogous to those observed earlier by Williams and co-workers for uncomplexed $[\text{BK} + 2\text{H}]^{2+}$.²¹ Both the loss of H_2O from the quasimolecular ion and the peptide bond cleavage producing $[\text{Arg-Pro} + \text{H}]^+$ and $[\text{Pro-Gly-Phe-Ser-Pro-Phe-Arg} + \text{H}]^+$ (b_2/y_7 pair) are the only products observed in the BIRD of both the complexed and isolated peptide. The cyclodextrin appears to have little influence on the fragmentation products suggesting a passive role of cyclodextrin as “solvent” in the peptide fragmentation reaction.

That only one specific moiety remains complexed to the cyclodextrin after fragmentation is intriguing. The presence of $[\text{CD}:\text{Arg-Pro} + \text{H}]^+$ suggests a strong ion-dipole interaction between the Arg¹ residue and the hydrophilic rims. The y_7 fragment that contains both Phe residues is observed only as a singly charged free peptide. As the fragmentation occurs while the peptide remains associated with the cyclodextrin, the preferential attachment of one fragment over the other implies a more favorable interaction between the b_2 fragment and the cyclodextrin than the y_7 fragment. Inspection of the peptide structure suggests a possible reason. Arg⁹ is less sterically accessible than Arg¹ because the Phe⁸ residue may interfere with the interaction of Arg⁹ and the cyclodextrin rim.

The peptide Lys¹-bradykinin (LBK) was chosen to observe the effect of a less basic residue in place of Arg¹. Some variation in the dissociation products was expected because the proton is not as strongly sequestered to the Lys residue. The hydrogen-deuterium exchange behavior of protonated lysine and arginine, an indicator of the intramolecular and intermo-

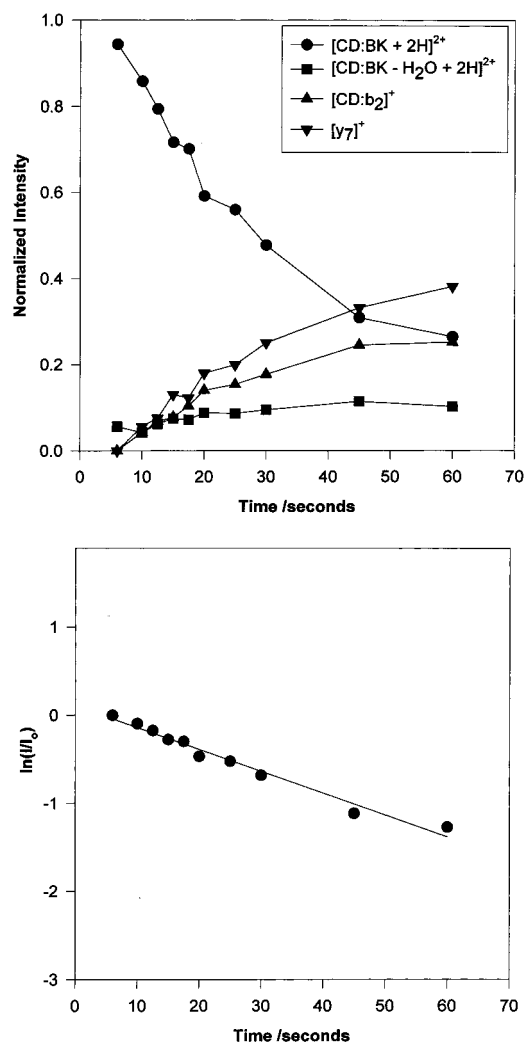


Figure 3. (a, top) Time dependence behavior of the relative intensity of $[\text{CD}:\text{BK} + 2\text{H}]^{2+}$ and fragment ions at 148 °C. (b, bottom) The semilog plot of the complex ion intensities.

lecular hydrogen bonding behavior of a molecule, is significantly different; LBK is more reactive toward H/D exchange with CH_3OD than BK.³⁰ The ionic fragments obtained from the photodissociation of $[\text{CD}:\text{LBK} + 2\text{H}]^{2+}$ are analogous to those observed with the BK complex (Scheme 2). The fragments correspond mainly to the b_2/y_7 pair with the cyclodextrin retained by the smaller (b_2) fragment. The product due to the loss of water is no longer present, while minor amounts of the singly charged peptide fragment, y_6 , are now observed (see also Figure 5). The major fragments indicate that the site of protonation remains the N- and the C-termini, even when the Arg residue is replaced with a less basic Lys residue. The Lys-Pro (b_2) fragment coordinates with CD while the remainder of the peptide is observed as a singly charged fragment.

The peptide GGBK was investigated for further comparison with BK and to assess the presence of gas-phase inclusion complexes with BK. In solution, the phenyl groups of BK are known to include into the cyclodextrin cavity. The phenyl group is absent in GGBK making it more difficult to form an inclusion complex with cyclodextrin. The CID threshold and the dissociation temperature from heated capillary experiments of the cyclodextrin complex suggest a stronger interaction between GGBK and cyclodextrin. The complex has a higher dissociation temperature and a higher dissociation threshold than does the BK complex.

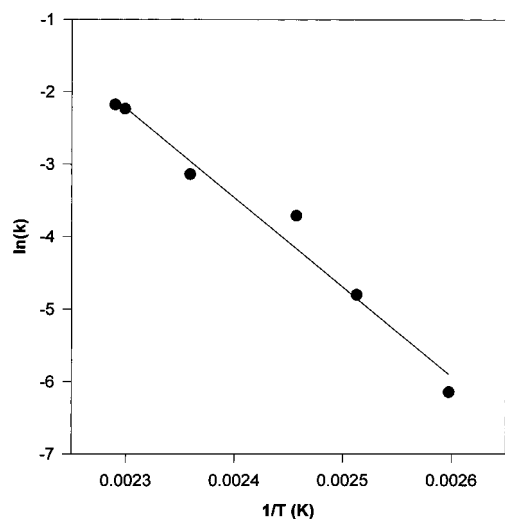


Figure 4. Arrhenius plot of the fragmentation of the $[\text{CD:BK} + 2\text{H}]^{2+}$ complex.

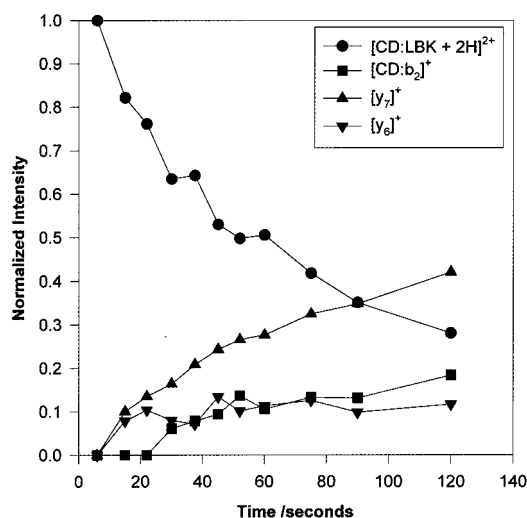
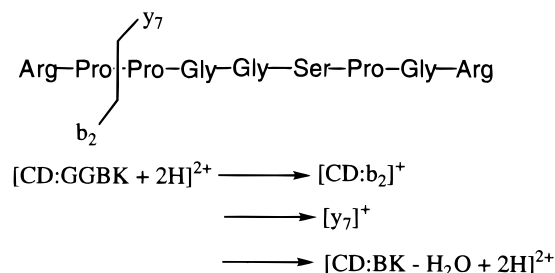


Figure 5. Time dependence behavior of the relative intensity of $[\text{CD:LBK} + 2\text{H}]^{2+}$ and fragment ions at 151 °C.

SCHEME 3: Fragmentation of $[\text{CD:GGBK} + 2\text{H}]^{2+}$ under BIRD Conditions



The photodissociation of the complex $[\text{CD:GGBK} + 2\text{H}]^{2+}$ produces fragments that are analogous to the BK complex (Scheme 3). As with the BK complex, only three fragments are observed, again corresponding to the loss of water and the peptide bond cleavage to yield the b_2/y_7 pair. The b_2 fragment is again coordinated to CD. If the inclusion complexes do form with BK and are left intact during ionization, it is not apparent from the comparison of the fragments produced by the two complexes.

When either Arg^1 or Arg^9 is removed, fragmentation of the peptide is less readily observed. With complexes of both dR1BK and dR9BK, the major products observed during

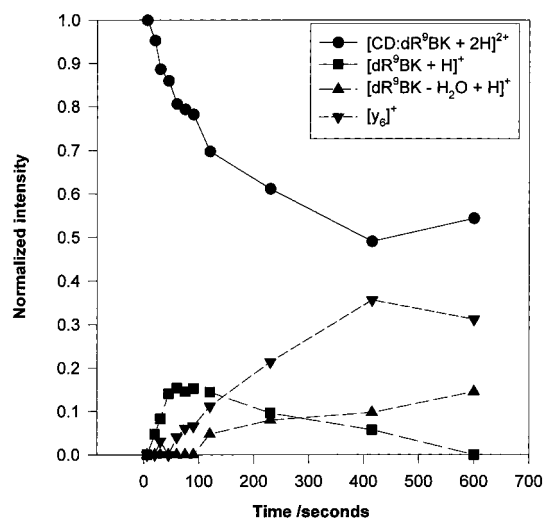


Figure 6. Time dependence behavior of the relative intensity of $[\text{CD:dR9BK} + 2\text{H}]^{2+}$ and fragment ions at 148 °C.

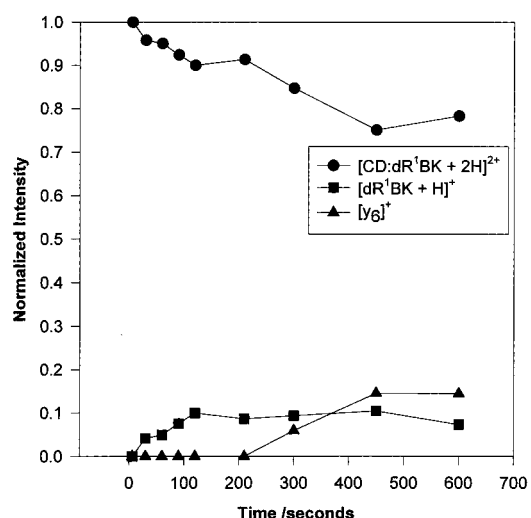
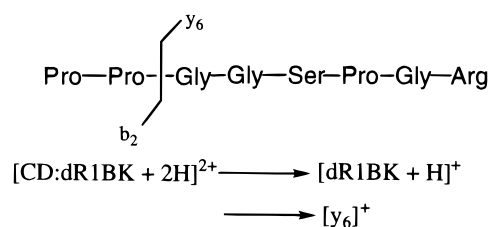


Figure 7. Time dependence behavior of the relative intensity of $[\text{CD:dR1BK} + 2\text{H}]^{2+}$ and fragment ions at 148 °C.

SCHEME 4: Fragmentation of $[\text{CD:DR1BK} + 2\text{H}]^{2+}$ under BIRD Conditions



photodissociation are the singly protonated peptides. The dR1BK complex produces one other product that corresponds to the singly charged y_6 fragment (Scheme 4). We believe this product to be a second-generation fragment resulting from the dissociation of the singly charged free peptide (see also Figure 7). The $[\text{CD:dR9BK} + 2\text{H}]^{2+}$ complex produces two additional products corresponding to the loss of water $[\text{dR9BK} - \text{H}_2\text{O} + \text{H}]^+$ and the y_6 fragment. These ions appear later and are likely produced by the dissociation of the isolated peptide.

The singly charged peptide products observed with dR1BK and dR9BK are essentially the same as those obtained by CID. We have postulated earlier that during CID the loss of charge is the result of a proton transfer between the complex and the

TABLE 1: E_a and A Values for the BIRD of a Number of Cyclodextrin Complexes of Bradykinin Analogues

peptide	E_a (eV)	A (s^{-1})	r^2	N
[BK + 2H] ²⁺ ^a	$0.84 \pm (0.04-0.1)$	1×10^8		
[CD:BK:CD + 2H] ²⁺	1.07 ± 0.09	2.3×10^{11}	0.98	4
[CD:Lys-1-BK + 2H] ²⁺	0.98 ± 0.10	1×10^{10}	0.92	4
[CD:des-Arg-1-BK + 2H] ²⁺	0.72 ± 0.20	1.5×10^6	0.99	3
[CD:des-Arg-9-BK + 2H] ²⁺	0.64 ± 0.20	5.8×10^6	0.91	3
[CD:Gly-5-Gly-8-BK + 2H] ²⁺	0.79 ± 0.20	9×10^7	0.85	5

^a Values obtained from ref 21.

background gas from the electrospray, i.e., either methanol or water. Unfortunately, the protonated products are too small to be observed with the current instrumental configuration. Charge disproportionation is another possibility. However, neither protonated cyclodextrins nor its fragments are observed, which suggests that the complex probably dissociates to a doubly charged peptide and a neutral cyclodextrin. The doubly charged peptide is further deprotonated by the background gas. The sites of protonation in isolated dR1BK are postulated by Kaltashov and Fenselau to be the Arg residue and the proline residue that makes up the N-terminus.³¹ In dR9BK, the protons are probably on the Arg¹ residue (N-terminus) and the Phe⁸ residue (C-terminus). In the complex, coordination of the peptide by cyclodextrin should not decrease the affinity of the Arg residue for protons; however, the second proton can be almost anywhere on the peptide backbone and not necessarily on the opposite end farthest away from the protonated Arg as the cyclodextrin can effectively coordinate and shield the second protonation site.

Kinetics of Reactions. The time dependence behavior of the complex [CD:BK + 2H]²⁺ at 148 °C is shown (Figure 3a). The semilog plot of the complex intensity is provided in Figure 3b to show first-order kinetics. Dissociation occurs immediately to produce the three major products: the loss of water, the singly charged Arg-Pro fragment coordinated to CD [CD:b₂]⁺, and the singly charged Pro-Gly-Phe-Ser-Pro-Phe-Arg fragment [y₇]⁺. No induction period was obtained, which was observed by Price et al.²² and attributed to the presence of ions at temperatures different from the analyzer ambient. For the [CD:BK + 2H]²⁺ complex, measurements at six temperatures were performed. From the rate constants, an Arrhenius plot was constructed (Figure 4) to yield an E_a of 1.07 ± 0.09 eV and an A of 2.3×10^{11} . Table 1 summarizes the activation energy (E_a) and the preexponential factor (A), derived from the Arrhenius plots of all five complexes. Included are the values obtained by Schnier et al. for the dissociation of the doubly charged bradykinin.²¹

The reaction kinetics of the LBK complex exhibit behavior similar to that of BK. The reaction profile at 151 °C (Figure 5) shows the rise in the intensity of the y₂/b₇ fragments as a function of time. The reaction is slightly slower as reflected by the small E_a and A values (0.98 eV and $1 \times 10^{10} s^{-1}$, respectively). The relatively less basic Lys¹ residue does not appear to change the dissociation barrier considerably, suggesting dissociation mechanisms that are similar.

The GGBK complex has a smaller activation barrier (0.79 eV), but the large error (0.2 eV) makes it difficult to ascertain whether the difference is real. The decay curves (not shown) at nearly all temperatures did not behave as well as either BK or LBK, and consequently the Arrhenius plot gave only satisfactory fit, $r^2 = 0.85$. These reactions were slow as reflected by the low A factor (9×10^7). At long reaction times (greater than 1 min), there is considerable ion loss, owing to the relatively low magnetic field, resulting in poor signal-to-noise at these reaction times. At higher temperatures, the decay

curves have appearances consistent with double exponentials. Attempts to correlate these curves to two-exponential functions, however, were not successful. We assume that the behavior of the curve is related to ion loss and that results in poor signal-to-noise rather than the presence of another dissociating pathway.

The dissociation of complexes of dR1BK and dR9BK involves extremely slow reactions. The reaction profile of [CD:dR9BK + 2H]²⁺ at 151 °C shows an initial rise of the singly charged peptide product (Figure 6). After about 50 s, the intensity of the singly charged y₆ fragment rises at the expense of the singly charged peptide. After 100 s, the fragment corresponding to the loss of water from the protonated peptide begins to gradually increase. The reaction profile of [CD:dR1BK + 2H]²⁺ shows primarily the singly charged peptide as the only product at early reaction times (≈ 10 s, Figure 7). At 300 s [y₇ + H]⁺ ion is again observed due also to the dissociation of the singly charge peptide. The slow reactivity of these complexes cannot be attributed to the activation barriers, 0.72 and 0.64 eV for dR1BK and dR9BK, respectively, but rather to the small preexponential factors ($10^6 s^{-1}$) that are indicative of entropically unfavorable and perhaps multistep rearrangement reactions.

Molecular Dynamics/Modeling Calculations. Three sets of calculations were performed. For each set, the lowest energy structures resulting from the 50 optimized structures were found to have similar features. For example, calculation 1 produced 19 structures that were within 5 kcal/mol of the lowest structure. All have important features similar to those shown in structure I. The representatives of the lowest energy structures of complexes derived from [CD:BK + 2H]²⁺ are presented in Chart 1. For clarity the peptide is represented by the stick model while the cyclodextrin is represented by the space-filling model. The Arg residues are in red, while the Phe residues are in blue.

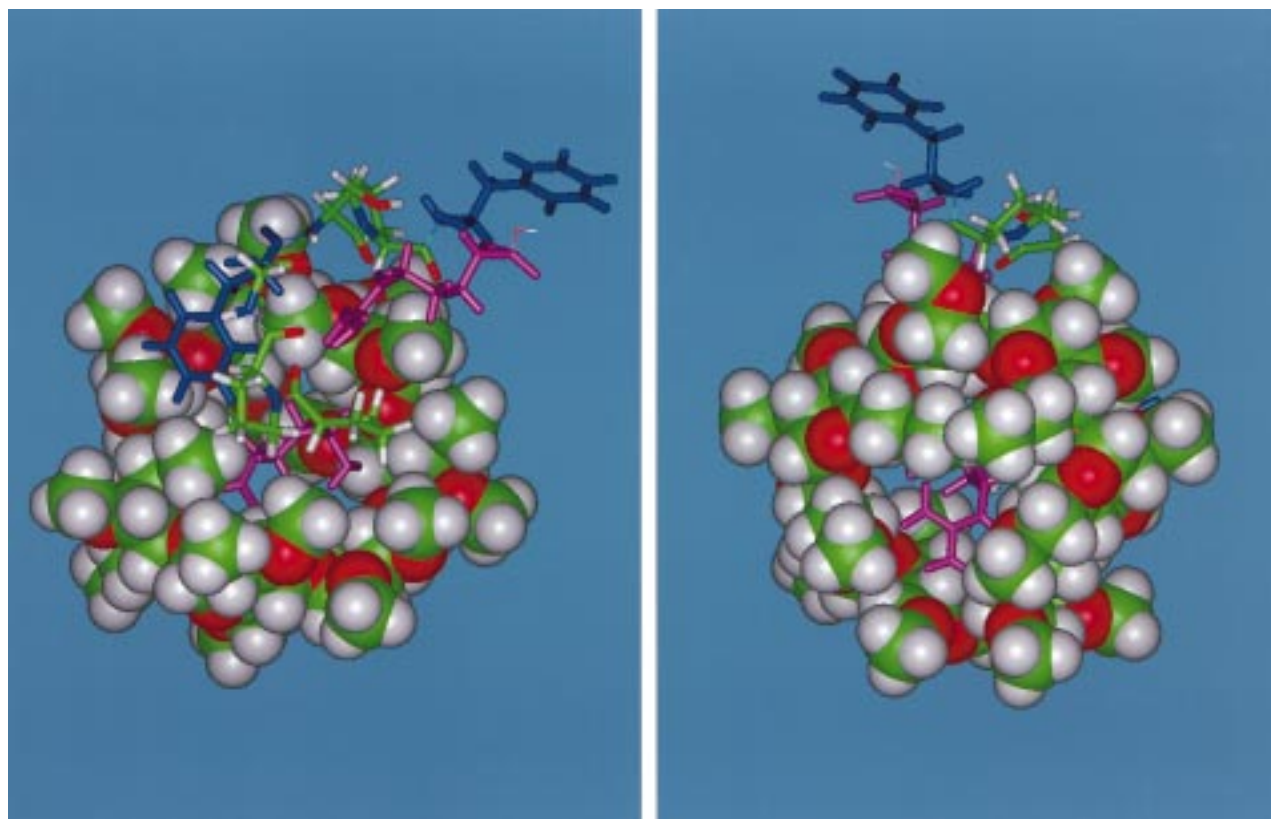
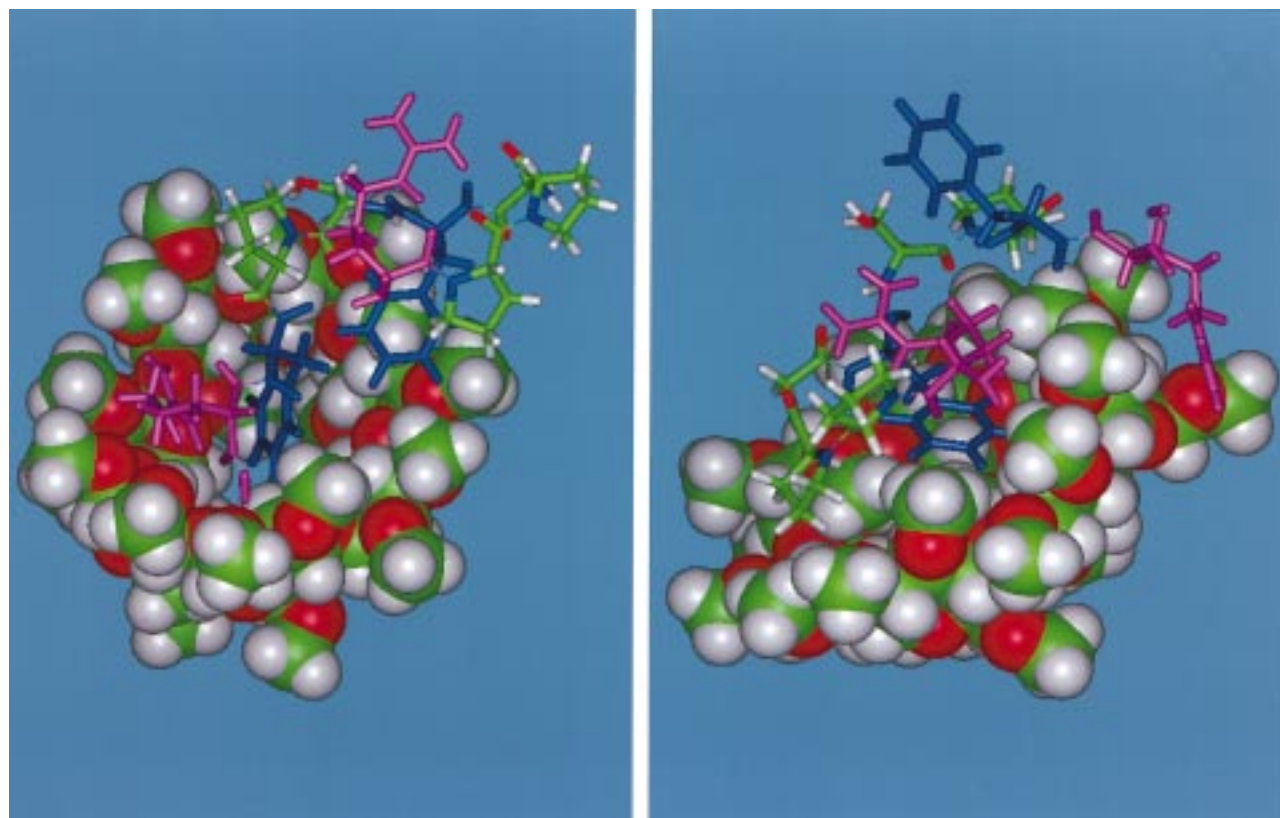
The lowest energy structure in the three sets of calculations involves inclusion of Arg¹ into the cavity (structures Ia and Ib). Despite the inclusion of Phe⁵ at the beginning of the calculation, Arg¹ has displaced Phe⁵ during the simulation. The resulting structure shows Arg¹ to be fully included in the cavity, with the positively charged guanido group interacting with the lower rim (bottom view, Ib). Arg⁹ similarly interacts with the upper rim; there appears little interaction between Phe⁵, Phe⁸ and the cyclodextrin.

The result of calculation 2 produced a structure where Phe⁸ remained included in the cyclodextrin cavity (structure II, Chart 2). However, the lowest energy structure resulting from the simulation is 17 kcal/mol less stable than I. Both Arg⁹ and Arg¹ also interact strongly with the upper rim.

Inclusion of Phe⁵ is maintained with softer annealing conditions in calculation 3 (III, Chart 2). The most favorable structure is 33 kcal/mol less stable than I. The phenyl group is not fully enveloped by the cavity, and the cyclodextrin appears more “bowl-like” with the wider rim made even wider. The open structure of the cyclodextrin maximizes interactions between Arg 1 and the upper rim. Note that Arg⁹ now interacts with the lower rim draping the remainder of the peptide on the outer surface of the cyclodextrin.

Discussion

Dissociation of Doubly Charged Complex. Complex dissociation (to intact peptide and cyclodextrin) and fragmentation (of the peptide or the cyclodextrin) are two competing pathways in the BIRD of the peptide–cyclodextrin complexes. For the three complexes of BK, LBK, and GGBK, complex dissociation

CHART 1: Structures Ia (left) and Ib (right)**CHART 2: Structures II (left) and III (right)**

is a less favorable process than peptide fragmentation. Given that the entropy of activation favors complex dissociation (as evidenced by the CID products), it follows that the activation energy for the dissociation will be higher than that for peptide fragmentation. This means that it may not be possible to obtain

the intrinsic energy of interaction between the peptides and the oligosaccharides using BIRD. In general, to obtain the energy of interactions in noncovalently bound complexes with BIRD, the moieties must not have a more favorable fragmentation pathway. The E_a for the fragmentation of bradykinin (1.07 eV)

in the complex still represents a lower limit for the strength of the peptide-saccharide interaction. This value is reasonable given the nature of the interaction between BK and CD. Essentially two protonated Arg residues (or one Lys and one Arg in LBK) interact with the cyclodextrin rims. An ion/dipole interaction involving protons produces between 0.5 and 1.5 eV of attraction.³²⁻³⁵ Two charge sites, such as two protonated Arg residues, interacting with the CD moiety can readily produce an interaction greater than 1.0 eV.

The activation barriers, preexponential factors, and fragment ions are all similar for BK and LBK. The largest observable difference is the presence of a minor y_7 fragment from the LBK complex. These similarities may indicate further similarities in the inter- and intramolecular interactions in the two complexes. Both Lys and Arg residues have high gas-phase basicities (230³⁶ and 245³⁷ kcal/mol, respectively); however, the reason for the high intrinsic basicity is very different. With Arg the high basicity is due to a single strongly basic site,³⁷ while in lysine it is due to a strong intramolecular interaction between two base sites of similar basicities.^{38,39} In the lysine amino acid the interaction involves mainly two amines, while in the peptide the amino side chain can also interact with a carbonyl amide form of the peptide backbone. In LBK, the protonated side chain has several avenues for intramolecular interactions. This means that in doubly charged BK the proton is more localized in the N- and C- termini than in LBK. The second proton in LBK has significant mobility, allowing it to interact with other basic positions. This is supported by H/D exchange experiments mentioned earlier that show doubly charged LBK is significantly more reactive to CH₃OD than doubly charged BK.³⁰ If the mechanism therefore involves some kind of proton motion (or a "mobile proton") as suggested by several groups, then one would expect LBK to be more reactive toward fragmentation than BK.^{40,41}

The results appear more consistent with a charge remote fragmentation reaction of the peptide.⁴²⁻⁴⁶ A charge-remote process has been postulated for the reaction of similar peptides but at significantly higher collision energies.⁴⁷ A charge site process depends on the position of the proton. To produce cleavage, protonation of the amide nitrogen is often invoked as the key step immediately preceding dissociation. The mobile proton mechanism involves the movement of the proton from the most basic site to the amide nitrogen. For bradykinin, this means shifting the proton from the highly basic side chain of Arg to the only mildly basic amide nitrogen (a difference of over 2 eV⁴⁸). This reaction should be less favorable with BK than the similar reaction involving the side chain of lysine. Instead, we find that both LBK and BK have similar activation barriers (0.98 and 1.07 eV, respectively). Furthermore, complexation of the peptide by cyclodextrin should make this reaction more difficult. The preexponential factor is sensitive to the entropy of the transition state, which may be strongly affected by the presence of the cyclodextrin. Instead, both BK and LBK complexes have A factors that are somewhat larger (2-3 orders of magnitude). Indeed, rather than a charge-site process, the reaction appears more consistent with a charge-remote process.

Inclusion and Interaction of the Peptide with Cyclodextrin. Molecular dynamics calculations predict that inclusion complexes are generally stable in the gas phase. If the complexes were initially formed in solution, then the inclusion complexes could be maintained in the gas phase depending on the initial inclusion configuration. It has been established that phenyl groups include into α -cyclodextrin (the six-membered

analog) and β -cyclodextrin in the solution.^{9,10,12,49-52} The molecular dynamics calculations predict that Phe⁸ (**II**) is more favorably included than Phe⁵ (**III**) in the gas phase. Nanosecond fluorescence spectroscopy studies show that several discrete species coexist in solution⁵³ so that species representing both forms of inclusion are probably present. However, NMR studies suggest that the inclusion is more effective if sufficient space exists for the high mobility of lipophilic guest moieties in the cavity.⁴⁹ This notion suggests that steric interactions in the cavity are important. That Phe⁸ is favored over Phe⁵, however, suggests that interactions at the rim are similarly important.

The fragmentation products offer few clues regarding the presence of gas-phase inclusion complexes. The major products observed from the dissociation of complexes of GGBK, LBK, and BK are all analogous. Inclusion of the phenyl groups of BK in cyclodextrin is similarly not immediately evident from the activation barriers or the preexponential factors. The peptide GGBK has a lower energy of activation and a lower preexponential factor than does BK (by 0.28 eV and 3 orders of magnitude, respectively). However, given the uncertainty in the values, these differences may not be significant. Furthermore, the possibility that the complexes rearrange to a non-inclusion intermediate before dissociation needs to be considered. The phenyl group may migrate out of the cyclodextrin cavity to a stable intermediate before the complex dissociates as predicted by the molecular dynamics simulations. The rearrangement may be the reason for the many similarities observed between the complexes of BK and GGBK.

Conclusions

The fragmentation reactions under blackbody radiation conditions suggest that covalent bond cleavages are, at least in these cases, more favorable than complex dissociation. Because many noncovalently bound complexes involve either peptides or proteins, peptide bond cleavage reactions may produce the major products in the dissociation of the respective complexes, making it inherently difficult to obtain the dissociation energies of the complexes. The results therefore suggest a limitation in using BIRD to determine the dissociation energies of noncovalently bound complexes.

However, the investigation of cyclodextrin complexes may provide a model for observing dissociation reactions in partially solvated systems. Cyclodextrin may play a similar role as that of alcohols in analogous reactions in the solution. Varying the derivatization of β -cyclodextrin, or other cyclodextrins, may provide systems for investigating the role of varying solvent polarities in peptide fragmentation reactions. These studies are currently underway.

Acknowledgment. Funding has been provided by the National Science Foundation (CHE-9310092). We thank Lisa R. Voss and Benjamin Garcia for help with the data analysis.

References and Notes

- (1) Katta, V.; Chait, B. T. *J. Am. Chem. Soc.* **1991**, *113*, 8534-5.
- (2) Ganem, B.; Li, Y.-T.; Henion, J. D. *J. Am. Chem. Soc.* **1991**, *113*, 6294-6.
- (3) Greig, M. J.; Gaus, H.; Cummins, L. L.; Sasmor, H.; Griffey, R. H. *J. Am. Chem. Soc.* **1995**, *117*, 10765-6.
- (4) Fen, R.; Castelano, A. L.; Billedeau, R.; Yuan, Z. *J. Am. Soc. Mass Spectrom.* **1995**, *6*, 1105-11.
- (5) Cheng, X.; Chen, R.; Bruce, J. E.; Schwartz, B. L.; Anderson, G. A.; Hofstadler, S. A.; Gale, D. C.; Smith, R. D. *J. Am. Chem. Soc.* **1995**, *117*, 8859-60.
- (6) Loo, R. R. O.; Goodlett, D. R.; Smith, R. D.; Loo, J. A. *J. Am. Chem. Soc.* **1993**, *115*, 4391-2.

- (7) Aplin, R. T.; Robinson, C. V.; Schofield, C. J.; Westwood, N. J. *J. Chem. Soc., Chem. Commun.* **1994**, 2415–6.
- (8) Rontoyianni, A.; Mavridis, I. M. *J. Inclusion Phenom. Mol. Recognit. Chem.* **1994**, 18, 211–27.
- (9) Rontoyianni, A.; Mavridis, I. M.; Hadjoudis, E.; Duisenber, A. J. M. *Carbohydr. Res.* **1994**, 252, 19–32.
- (10) Szejtli, J. *Cyclodextrins and Their Inclusion Complexes*; Akadémiai Kiadó: Budapest, 1982; p 296.
- (11) Szejtli, J. *Pharm. Technol. Int.* **1991**, 3, 16–20.
- (12) Hirai, H.; Shiraishi, Y.; Mihori, H.; Kawamura, T. *Polymer J.* **1995**, 27, 1064–7.
- (13) Letellier, S.; Maupas, B.; Gramond, J. P.; Guyon, F.; Gareil, P. *Anal. Chim. Acta* **1995**, 315, 357–63.
- (14) Korkas, P. P.; Weber, E.; Czugler, M.; Narayszabo, G. *J. Chem. Soc., Chem. Commun.* **1995**, 21, 2229–30.
- (15) Cunniff, J. B.; Vouros, P. *J. Am. Soc. Mass Spectrom.* **1995**, 6, 437–47.
- (16) Camilleri, P.; Haskins, N. J.; New, A. P.; Saunders, M. R. *Rapid Commun. Mass Spectrom.* **1993**, 7, 949–52.
- (17) Selva, A.; Redenti, E.; Pasini, M.; Ventura, P.; Casetta, B. *J. Mass Spectrom.* **1995**, 30, 219–20.
- (18) Penn, S. G.; He, F.; Green, M. K.; Lebrilla, C. B. *J. Am. Soc. Mass Spectrom.* **1997**, 8, 244–52.
- (19) Dunbar, R. C.; McMahon, T. B.; Thölmann, D.; Tonner, D. S.; Salahub, D. R.; Wei, D. *J. Am. Chem. Soc.* **1995**, 117, 12819–25.
- (20) Thölmann, D.; Tonner, D. S.; McMahon, T. B. *J. Phys. Chem.* **1994**, 98, 2002–4.
- (21) Schnier, P. D.; Price, W. D.; Jockusch, R. A.; Williams, E. R. *J. Am. Chem. Soc.* **1996**, 118, 7178–89.
- (22) Price, W. D.; Schnier, P. D.; Williams, E. R. *Anal. Chem.* **1996**, 68, 859–66.
- (23) McCullough, S. M.; Gard, E.; Lebrilla, C. B. *Int. J. Mass Spectrom. Ion Processes* **1991**, 107, 91–102.
- (24) Gard, E. E.; Green, M. K.; Warren, H.; Camara, E. J. O.; He, F.; Penn, S. G.; Lebrilla, C. B. *Int. J. Mass Spectrom. Ion Processes* **1996**, 158, 115–27.
- (25) Carroll, J. A.; Ngoka, L.; McCullough, S. M.; Gard, E.; Jones, A. D.; Lebrilla, C. B. *Anal. Chem.* **1991**, 63, 2526–9.
- (26) Loo, J. A.; Edmonds, C. G.; Smith, R. D. *J. Am. Chem. Soc.* **1993**, 65, 425–38.
- (27) Carroll, J. A.; Wu, J.; Do, T. A.; Lebrilla, C. B. Unpublished results, 1994.
- (28) Ngoka, L.; Lebrilla, C. B. *J. Am. Soc. Mass Spectrom.* **1993**, 4, 210–5.
- (29) Ngoka, L. C.; Gal, J. F.; Lebrilla, C. B. *Anal. Chem.* **1994**, 66, 692–8.
- (30) Green, M. K.; Lebrilla, C. B. *Int. J. Mass Spectrom.*, in Press.
- (31) Kaltashov, I. A.; Fenselau, C. C. *J. Am. Chem. Soc.* **1995**, 117, 9906–10.
- (32) Meot-Ner, M. *J. Am. Chem. Soc.* **1983**, 105, 4912–5.
- (33) Meot-Ner, M. *J. Am. Chem. Soc.* **1984**, 106, 257–64.
- (34) Hiraoka, K.; Takimoto, H.; Yamabe, S. *J. Phys. Chem.* **1986**, 90, 5910–4.
- (35) Schnier, P. D.; Price, W. D.; Strittmatter, E. F.; Williams, E. R. *J. Am. Soc. Mass Spectrom.* **1997**, 8, 771–80.
- (36) Lias, S. G.; Liebman, J. F.; Levin, R. D. *J. Phys. Chem. Ref. Data* **1984**, 13, 695–808.
- (37) Wu, Z.; Fenselau, C. *Rapid Commun. Mass Spectrom.* **1992**, 6, 403–5.
- (38) Bliznyuk, A. A.; Schaefer, H. F., III; Amster, I. J. *J. Am. Chem. Soc.* **1993**, 115, 5149–54.
- (39) Wu, Z.; Fenselau, C. *Rapid Commun. Mass Spectrom.* **1994**, 8, 777–80.
- (40) Dongré, A. R.; Somogyi, A.; Wysocki, V. *J. Mass Spectrom.* **1996**, 31, 339–50.
- (41) Burlet, O.; Orkiszewski, R. S.; Gaskell, S. J. *J. Am. Soc. Mass Spectrom.* **1993**, 4, 470–6.
- (42) Adams, J. *Mass Spectrom. Rev.* **1990**, 9, 141.
- (43) Hensen, N. J.; Tomer, K. B.; Gross, M. L. *J. Am. Chem. Soc.* **1985**, 107, 1863.
- (44) Wysocki, V. H.; Bier, M. E.; Cooks, R. G. *Org. Mass Spectrom.* **1988**, 23, 627.
- (45) Tomer, K. B.; Crow, F. W.; Gross, M. L. *J. Am. Chem. Soc.* **1983**, 105, 5487.
- (46) Hayes, R. N.; Gross, M. L. In *Methods in Enzymology*; McCloskey, J. A., Ed.; Academic Press: San Diego, CA, 1990; Vol. 193; pp 237–63.
- (47) Kaltashov, I. A.; Fenselau, C. *Int. J. Mass Spectrom. Ion Processes* **1997**, 160, 331–8.
- (48) Wu, J.; Lebrilla, C. B. *J. Am. Chem. Soc.* **1993**, 115, 3270–5.
- (49) Schneider, H. J.; Blatter, T.; Simova, S. *J. Am. Chem. Soc.* **1991**, 113, 1996–2000.
- (50) Pitha, J.; Milecki, J.; Fales, H.; Pannell, L.; Eukama, K. *Int. J. Pharm.* **1986**, 29, 73–82.
- (51) Pena, A. M. d. I.; Ndou, T. T.; Zung, J. B.; Greene, K. L.; Live, D. H.; Warner, I. M. *J. Am. Chem. Soc.* **1991**, 113, 1572–7.
- (52) Haskins, N. J.; Saunders, M. R.; Camilleri, P. *Rapid Commun. Mass Spectrom.* **1994**, 8, 423–6.
- (53) Bright, F. V.; Catena, G. C.; Huang, J. *J. Am. Chem. Soc.* **1989**, 112, 1343.